

AD-A197 248

2

SACLANTCEN REPORT
serial no.: SR-116

SACLANT ASW
RESEARCH CENTRE
REPORT

DTIC FILE COPY



**Properties of beam-noise
fluctuations for horizontal arrays
in ship-induced noise fields**

R. Heitmeyer

DTIC
ELECTE
S JUN 30 1988 D

April 1988

The SACLANT ASW Research Centre provides the Supreme Allied Commander Atlantic (SACLANT) with scientific and technical assistance under the terms of its NATO charter, which entered into force on 1 February 1963. Without prejudice to this main task—and under the policy direction of SACLANT—the Centre also renders scientific and technical assistance to the individual NATO nations.

This document has been approved
for public release and sale in
distribution is unlimited.

88 6 29 170

This document is released to a NATO Government at the direction of SACLANT ASW Research Centre subject to the following conditions:

- The recipient NATO Government agrees to use its best endeavours to ensure that the information herein disclosed, whether or not it bears a security classification, is not dealt with in any manner (a) contrary to the intent of the provisions of the Charter of the Centre, or (b) prejudicial to the rights of the owner thereof to obtain patent, copyright, or other like statutory protection therefor.
- If the technical information was originally released to the Centre by a NATO Government subject to restrictions clearly marked on this document the recipient NATO Government agrees to use its best endeavours to abide by the terms of the restrictions so imposed by the releasing Government.

Page count for SR-116
(excluding covers)

Pages Total	
i-iv	4
1-42	42
<hr/>	
46	

SACLANT ASW Research Centre
Viale San Bartolomeo 400
19026 San Bartolomeo (SP), Italy

tel: 0187 540 111
telex: 271148 SACENT I

NORTH ATLANTIC TREATY ORGANIZATION

SACLANTCEN SR-116

Properties of beam-noise
fluctuations for
horizontal arrays in
ship-induced noise fields

R. Heitmeyer

The content of this document pertains
to work performed under Project 21 of
the SACLANTCEN Programme of Work.
The document has been approved for
release by The Director, SACLANTCEN.



Peter C. Wille
Director

SACLANTCEN SR-116

- ii -

intentionally blank page

**Properties of beam-noise fluctuations for
horizontal arrays in ship-induced noise
fields**

R. Heitmeyer

Abstract: This report describes properties of the cumulative distribution function for the beam noise observed on a horizontal array operating in a ship-induced noise field. The beam-noise distribution is determined using a Poisson shipping noise model and related to the system characteristics and the noise environment through six physical parameters: the directivity, the sidelobe degradation, the sidelobe/mainlobe power ratio, the noise anisotropy, the isotropic shipping level and the shipping anisotropy. The results indicate that the beam-noise distribution function takes two different forms depending on the extent to which the noise contributions from individual ships are resolved. For highly resolved shipping, the distribution function describes fluctuations that range from very low values to very high values. The low noise values are characterized by a 'noise floor' which represents the lowest noise value that is visible a significant percentage of the time regardless of the extent of the shipping resolution. The value of the noise floor increases linearly with the sidelobe/mainlobe power ratio and the sidelobe degradation and decreases linearly with the noise anisotropy. The percentage of time that the noise floor is visible increases with the directivity and decreases with the shipping anisotropy and the logarithm of the isotropic shipping level. For weakly resolved shipping, the distribution function describes comparatively small beam-noise fluctuations. The range of low noise values that are visible, as determined by the lower tail of the distribution, increases with the directivity and decreases with the shipping anisotropy and the shipping level and is essentially independent of the sidelobe degradation and the noise anisotropy. The transition from weakly resolved shipping to highly resolved shipping occurs for a 2.3 dB increase in the directivity, a 2.3 dB decrease in the shipping anisotropy, or a 58% decrease in the isotropic shipping level. For both highly resolved and weakly resolved shipping, the percentage of time that high noise values occur is only weakly dependent on the model parameters.

Keywords: beam noise ◦ cumulative distribution ◦ directivity ◦ horizontal arrays ◦ noise anisotropy ◦ ship-induced noise ◦ shipping anisotropy ◦ sidelobe degradation

Contents

1. Introduction 1
2. Noise model overview and parameter specification 4
3. Beam-noise distribution examples 10
4. The beam-noise model approximations 15
5. Examples 24
6. Summary and conclusions 29

References 31

Appendix A - Noise model equations 33
Appendix B - Derivations of the model parameters 36
Appendix C - Examples of shipping and noise environments . . . 41



Accession For	
NTIS GRA&I	<input checked="" type="checkbox"/>
DTIC TAB	<input type="checkbox"/>
Unannounced	<input type="checkbox"/>
Justification	
By _____	
Distribution/	
Availability Codes	
Dist	Avail and/or Special
A-1	

1. Introduction

The design and deployment of horizontal array systems requires a thorough understanding of how the time-averaged beam noise depends on the characteristics of the system and the noise environment in which it operates. For many noise fields an understanding of the mean value of the beam noise may be adequate, since for the averaging times of interest the fluctuations in the beam noise with respect to the mean are not significant. For ship-induced noise fields, however, large fluctuations in the beam noise can occur from one averaging period to another. These fluctuations result from the fact that the beam noise observed during an averaging period is largely due to the contributions from the ships that lie in the mainlobe sector of the beam pattern during that averaging period. As time progresses different ships with different source level characteristics pass through the mainlobe sector at different ranges from the array site. This can result in large variations in the received contributions from the ships in the mainlobe sector, and hence large fluctuations in the beam noise from one averaging period to another. When this is the case an understanding of the dependence of both the beam-noise fluctuations and the mean beam noise can be important to the effective use of the system.

The dependence of the mean beam noise on the system and the noise environment is well known. The noise environment is described by an angular noise distribution which represents the mean noise per degree bearing as a function of the bearing angle. This function is determined by the mean distribution of the shipping relative to the site, the mean acoustic transmission loss in the directions of the shipping, and the mean source level spectrum of that shipping. The mean beam noise is determined as the integral of the angular noise distribution and the beam pattern with respect to the bearing angle. In many situations this integral is well-approximated by the product of the beamwidth and the angular noise distribution in the direction of the beam steering angle. In these cases, the mean beam noise increases linearly with the angular noise power and decreases linearly with the directivity. Considerable effort has been directed towards determining the angular noise distribution for specific noise environments and predicting the mean beam noise for particular array systems.

Clearly, the fluctuations in the beam noise depend on the averaging time. For many applications it is reasonable to assume that the averaging time is short compared with the time required for ships to move into or out of the mainlobe sector of the beam pattern. Under this assumption the beam-noise fluctuations can be decomposed into two components—a long-term component that describes the fluctuations in the beam noise from one averaging period to another and that result from the motion of the ships into and out of the mainlobe sector, and a short-term component that describes the fluctuations due to the ships that are actually present in the mainlobe sector during each averaging period. The former is largely determined by

the source-level spectra and the transmission loss characteristics for the ensemble of ships that pass through the mainlobe sector. The latter is largely determined by the fluctuations in the source-level of the ships present in the mainlobe sector during the averaging period and the fluctuations in the transmission loss that results from the small motions of those ships during the averaging period. The extent of these fluctuations, which decreases with the averaging time, is usually small compared to that of the long-term fluctuations provided that the averaging time is not too short. In this report we consider only the long-term component of the fluctuations.

In heuristic terms, the extent of the beam-noise fluctuations is related to the extent to which individual ships are resolved in steering angle. Large fluctuations in the beam noise occur for systems and environments where a number of individual ships are resolved in steering angle. This is because ships can only be resolved if there is a significant percentage of time when either no ship lies in the mainlobe sector or at most one ship lies in the mainlobe sector. During these periods the beam noise fluctuates between high values which occur when a ship lies in the mainlobe sector and low values which occur when no ships lie in the mainlobe sector. For systems and environments with highly resolved shipping, the contributions from the ships in the sidelobe sectors are important, since these contributions determine the low noise values. At the other extreme comparatively small fluctuations in the beam noise occur when individual ships are not resolved. This is because ships are not resolved only if a number of ships are present in the mainlobe sector essentially all of the time. Under this condition, the fluctuations are small since the large contributions from some of the ships in the mainlobe sector tend to be offset by small contributions from other ships in the mainlobe sector. Extreme fluctuations in the beam noise occur only rarely; low noise values occur only when there are no ships in the mainlobe sector or when the contributions from all of the ships in the mainlobe sector are small; high noise values occur only when the contribution from one of the ships is large enough to dominate the contributions from the remaining ships. For systems and environments with low shipping resolution, the contributions from ships in the sidelobe sectors are not important since the beam noise is almost always determined by the contributions from the ships in the mainlobe sector. Factors that determine the extent of the shipping resolution and hence the extent of the beam-noise fluctuations are the beamwidth and the number of ships in the direction of the beam. Factors that determine the sidelobe contributions and hence control the low noise values for highly resolved shipping are the sidelobe level of the beam pattern and the angular noise distribution in the directions of the sidelobe sectors.

In this report we present a quantitative description of the effects of the system characteristics and the noise environment on the extent of the beam-noise fluctuations. The fluctuations are described by their cumulative probability distribution function and the beam-noise percentile determined from this distribution function. These quantities are determined from a beam-noise model that describes the system and the noise environment in terms of six parameters. Three of these parameters, the directivity index, the ideal sidelobe-to-mainlobe noise power ratio, and the sidelobe

degradation, characterize the system. The directivity index and the ideal sidelobe-to-mainlobe noise power ratio, hereafter referred to simply as the directivity and the ideal sidelobe/mainlobe ratio respectively, are defined for an array/beamforming system in the absence of degradation. These parameters are determined by the array length, the beam steering angle, the frequency and the spatial shading function used in the beamformer. The sidelobe degradation specifies any degradation in the actual beam pattern that results from phase and amplitude errors, hydrophone position errors, and missing or defective hydrophones, etc. The remaining three parameters, the isotropic shipping level, the shipping anisotropy and the noise anisotropy, describe the mean properties of the noise environment. The isotropic shipping level specifies the mean number of ships in the region per degree bearing as if those ships were isotropically distributed with respect to the array site; the shipping anisotropy specifies the angular variation in the mean number of ships relative to the isotropic level. The noise anisotropy specifies the angular noise distribution relative to the isotropic noise level. The directivity, the isotropic shipping level and the shipping anisotropy determine the extent of the shipping resolution; the ideal sidelobe/mainlobe ratio, the sidelobe degradation and the noise anisotropy determine the extent of the sidelobe contributions.

The report is organized as follows. Section 2 presents a brief description of the beam-noise model and formal definitions of the six physical parameters in terms of the components of that model. In Sect. 3 we present numerical examples of the beam-noise distribution function that illustrate the effect of the shipping resolution and the sidelobe contributions using the directivity as the ship resolution parameter and the sidelobe degradation as the sidelobe contribution parameter. These examples provide both the motivation for much of the terminology used in the report and a means of illustrating the dependence of the distribution function on the remaining physical parameters. In Sect. 4 we present approximations that are derived from the beam-noise model. These approximations are used to both extend the results of Sect. 3 to the other model parameters and to obtain estimates for the salient characteristics of the distribution function in terms of the model parameters. In addition, we present a formal definition of weakly resolved and highly resolved shipping as a means of identifying the model parameters that lead to the different forms for the distribution function observed in the examples of Sect. 3. Finally, in Sect. 5 we illustrate the application of the results of Sect. 4 by using those results in conjunction with numerical examples to describe the dependence of the beam-noise fluctuations on the array heading for certain canonical noise environments.

2. Noise model overview and parameter specification

The beam-noise model is based on two fundamental assumptions—a superposition assumption and a Poisson shipping assumption. The superposition assumption states that the total noise intensity is obtained as the sum of the noise intensity contributions from the individual ships that produce the noise. Because of this assumption the model can only be used to describe the fluctuations in the beam noise at the output of a time-averager, since it is only through time averaging that a superposition assumption can hold for the noise intensity contributions. For most averaging times of interest this assumption will be satisfied to within acceptable limits. The Poisson shipping assumption states that the tracks of the individual ships can be described in terms of the positions of those ships at some arbitrary reference time and that those positions are distributed throughout the region according to a Poisson process. The Poisson process is determined by a shipping density $D(r, \theta)$ which represents the mean number of ships per unit area at a range r and bearing θ measured from the array site. Figure 1 shows an example of a linear array located at a fixed site in a region and one possible set of ship tracks that satisfy a Poisson shipping assumption for that region. The dots show the positions of the ships at the reference time; the arrowheads show the positions of the ships at some future time. Note that the range and bearing dependence in the shipping density is necessary to represent the fact that ships are usually not distributed uniformly throughout the region.

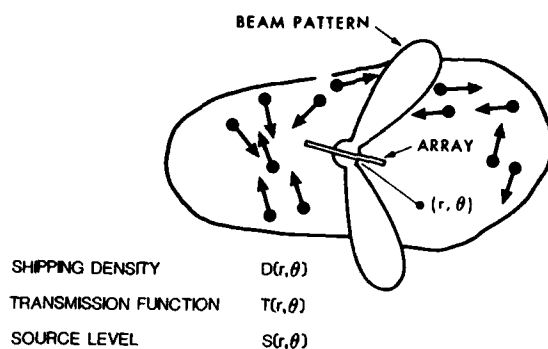


Fig. 1. A possible set of ship tracks seen by an array.

From these assumptions, it is shown in [1] that the distribution function for the beam noise at any arbitrary time can be determined from the shipping density and the probability density of the noise contribution from an individual ship. The noise contribution from a ship, which depends on the location of that ship, is determined from a transmission loss $T(r, \theta)$, a source level $S(r, \theta)$ and the array beam pattern, each expressed in a linear as opposed to a decibel scale. The transmission loss consists of a deterministic component which represents the 'smooth' variations in the transmission loss with range and bearing, and a stochastic component which represents the fluctuations with respect to the smooth component. The source-level is a random variable that represents the source level for the aggregate of all ships that pass through the point (r, θ) . For reference purposes, the basic equations specifying the model are presented in Appendix A. Other beam-noise fluctuation models based on the Poisson shipping assumption are described in [2] and [3]. It is emphasized that these models are not based on a continuum assumption on the ship locations; such an assumption would not be plausible in the light of the sparse distribution of ships in most regions. Furthermore, in these models the calculation of the distribution function does not require knowledge of the tracks of the individual ships. An example of a shipping density for the Mediterranean Sea can be found in [4].

The model implementation determines the distribution function for the total beam noise in terms of the distribution function for the fluctuating component. The fluctuating component, which is denoted here by B and referred to simply as the beam noise, is expressed in a decibel scale and normalized to have unit mean when expressed in a linear scale, i.e. $E[10^{B/10}] = 1$. As such, the total beam noise, B_T , is the decibel sum of B and the mean beam noise B_m where $B_m = 10 \log(E[10^{B_T/10}])$. Note that with this normalization, low noise values, $B < 0$ and $B_T < B_m$, are low in comparison with means taken on a linear scale, not in comparison with means taken on a decibel scale. That this is the case follows from the fact that $E[B] < 10 \log(E[10^{B/10}]) = 0$ and $E[B_T] < 10 \log(E[10^{B_T/10}]) = B_m$.

The parameterization of the model described in Sect. 1 is obtained under the additional assumption that the array beam pattern can be approximated by a two-valued beam pattern. The two-valued approximation is illustrated in Fig. 2a as a function of the planewave incident angle θ' for a fixed value of the beam steering angle θ_s , where both are measured from the front of the array. This beam pattern has the form

$$B_A(\theta', \theta_s) = \begin{cases} 1, & \text{for } \theta' \text{ in } \text{BW}(\theta_s) \\ 10^{S_d/10}, & \text{for } \theta' \text{ in } \text{BW}_s(\theta_s), \end{cases} \quad (1)$$

where the mainlobe sector BW is the angular sector of width BW centered in the steering direction θ_s , the sidelobe sector BW_s is determined by the condition, $\text{BW} \cup \text{BW}_s = [0, \pi]$ and S_d is the sidelobe level expressed in decibels.

The parameters for the beam pattern approximation, the beamwidth BW and the sidelobe level S_d , are chosen so that for a planar isotropic noise field, both the approx-

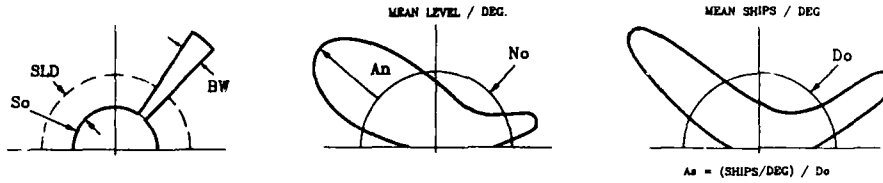


Fig. 2. Illustrations of the model parameters as a function of θ' : (a) beam pattern approximation; (b) angular noise distribution, noise anisotropy and isotropic noise level; (c) angular shipping distribution, shipping anisotropy and isotropic shipping level.

imation and the actual beam pattern yield identical values of the mean beam noise and the sidelobe/mainlobe ratio. Under these constraints, expressions for BW and S_d can be derived which relate these parameters to the three system parameters—the directivity DI, the ideal sidelobe/mainlobe ratio B_{s_0} , and the sidelobe degradation SLD. The directivity and the ideal sidelobe/mainlobe ratio are defined in terms of the actual beam pattern for the system with no degradation, $B_{A_0}(\theta', \theta_s)$. The directivity, which represents the array gain for a planewave signal and the planar isotropic noise field, is defined in the usual way by

$$DI = 10 \log(\pi / BW_0), \quad (2a)$$

where

$$BW_0(\theta_s) = \int_0^\pi B_{A_0}(\theta', \theta_s) d\theta' \quad (2b)$$

is the beamwidth for the system in the absence of degradation. The ideal sidelobe/mainlobe ratio B_{s_0} represents the ratio of the mean noise in the sidelobe sector BW_{s_0} to that in a mainlobe sector BW_0 , where BW_0 has angular width BW_0 and the definition of BW_{s_0} is analogous to that of BW_s . The defining equation for the ideal sidelobe/mainlobe ratio is

$$B_{s_0} = 10 \log \left[\frac{\int_{BW_{s_0}} B_{A_0}(\theta', \theta_s) d\theta'}{\int_{BW_0} B_{A_0}(\theta', \theta_s) d\theta'} \right], \quad (3)$$

The actual beam pattern for the degraded system, $B_{A_d}(\theta', \theta_s)$, is taken to be the mean value of the beam pattern that results from statistically independent channel-to-channel errors. Under this assumption, it is shown in Appendix B that the sidelobe level S_d is related to the sidelobe degradation parameter by

$$S_d = S_0 + \text{SLD}, \quad (4)$$

where S_0 is the sidelobe level determined by the ideal beam pattern $B_{A_0}(\theta', \theta_s)$. For realistic degradations and typical values of DI and B_{s_0} , $BW \doteq BW_0$, $S_0 \doteq B_{s_0} - DI$ and $S_d \doteq B_{s_0} - DI + SLD$. The exact expressions for BW , S_0 and S_d are given in Appendix B along with the expression relating SLD to a parameter describing the channel-to-channel errors.

To compute the directivity and the sidelobe/mainlobe ratio for a particular beam pattern $B_{A_c}(\theta', \theta_s)$, the beamwidth BW_0 is first obtained numerically from Eq. (2b). The directivity follows immediately from Eq. (2a) and the sidelobe/mainlobe ratio is obtained numerically from Eq. (2) with the mainlobe and the sidelobe sectors determined by BW_0 . In general for equally spaced arrays, the beamwidth BW_0 , and hence the directivity and the ideal sidelobe/mainlobe ratio, depend on the frequency, the steering angle, the length of the array and the shading function used in the beamformer. In the special case where the frequency, the steering angle and the shading function are fixed, it can be shown by direct computation that the ideal sidelobe/mainlobe ratio is essentially independent of the length of the array, provided that the number of hydrophones is not too small. Thus in the special case where the system parameters are used to describe the effect of array length on the beam-noise fluctuations only the directivity and the sidelobe degradation need be considered.

The remaining three parameters—the noise anisotropy, the shipping anisotropy, and the isotropic shipping level—are used to represent an anisotropic noise field and a non-uniform shipping density for the two-valued beam pattern. In addition to these parameters, a seventh parameter, the isotropic noise level, is needed to determine the mean beam noise. All of these parameters are determined from the angular noise distribution $n(\theta)$ and an angular shipping distribution $d(\theta)$. The angular noise distribution is determined from the model components by

$$n(\theta) = \int_{R(\theta)} D(r, \theta) \bar{S}(r, \theta) \bar{T}(r, \theta) dA(r), \quad (5)$$

where $\bar{S}(r, \theta)$ and $\bar{T}(r, \theta)$ are the mean transmission loss and the mean source level respectively, $dA(r)$ is the differential range element for a spherical earth and $R(\theta)$ is the range set containing all of the ships that can be heard at the array site in the direction θ , i.e., $R(\theta) = \{r; D(r, \theta) \bar{T}(r, \theta) > 0\}$. The angular shipping distribution represents the mean number of ships per degree bearing relative to the array site. This function, which depends only on the spatial shipping density $D(r, \theta)$, is defined by

$$d(\theta) = \int_{R(\theta)} D(r, \theta) dA(r). \quad (6)$$

The isotropic noise level N_0 and the isotropic shipping level D_0 are simply the twice the averages of the corresponding angular distributions with respect to bearing.

The noise anisotropy and the shipping anisotropy describe the corresponding angular distributions as seen through the mainlobe sector of the beam pattern. For a given

array heading θ_h and beam steering angle θ_s , the noise anisotropy $A_N(\theta_h, \theta_s)$ is obtained by folding the angular noise distribution about the array axis, averaging the result over the mainlobe sector and dividing by the isotropic noise level. The defining equations are

$$A_N(\theta_h, \theta_s) = 10 \log \left[\text{BW}(\theta_s)^{-1} \int_{\text{BW}(\theta_s)} n_F(\theta', \theta_h) / N_0 d\theta' \right], \quad (6a)$$

where

$$n_F(\theta'; \theta_h) = n(\theta_h - \theta') + n(\theta_h + \theta') \quad (6b)$$

is the folded angular noise distribution. The shipping anisotropy, which is obtained in an analogous manner, is defined by

$$A_S(\theta_h, \theta_s) = 10 \log \left[\text{BW}(\theta_s)^{-1} \int_{\text{BW}(\theta_s)} d_F(\theta'; \theta_h) / D_0 d\theta \right], \quad (7a)$$

where

$$d_F(\theta'; \theta_h) = d(\theta_h - \theta') + d(\theta_h + \theta') \quad (7b)$$

is the folded angular shipping distribution. The equations for the sidelobe/mainlobe ratio, the mean beam noise and the array gain for the two-valued beam pattern with sidelobe degradation and an anisotropic noise field are contained in Appendix B.

In general, both the noise anisotropy and the shipping anisotropy depend on the directivity DI and the ideal sidelobe/mainlobe ratio B_{s0} , since these parameters determine the width of the mainlobe sector. However, for systems with reasonably large directivities, the beamwidth is small enough that the average over the mainlobe sector in Eqs. 6a and 7a is approximately equal to the value of the folded angular distribution in the direction of the steering angle. Thus, for systems with reasonable directivities, $A_N \doteq 10 \log[n_F(\theta_s; \theta_h) / N_0]$ and $A_S \doteq 10 \log[d_F(\theta_s; \theta_h) / D_0]$, and hence the anisotropies depend on the system only through the beam steering angle and the array heading. For these systems the anisotropies can be obtained directly from the corresponding angular distributions, provided that these distributions are known. For a fixed steering angle, θ_{s0} , the anisotropies are obtained by summing the corresponding angular distribution in the directions of the two beam pointing angles, $\theta_p = \theta_h \pm \theta_{s0}$, dividing by the appropriate isotropic level and expressing the result in a decibel scale. For a fixed array heading θ_{h0} , the anisotropies are obtained by folding the corresponding angular distribution about the array axis, expressing the result as a function of steering angle and dividing by the appropriate isotropic level. An example of the dependence of the anisotropies on the steering angle is illustrated in the plots of Figs. 2b and 2c. In these plots the folded angular distributions and the isotropic levels are expressed in a decibel scale as a function of the steering angle and hence the anisotropy is simply the difference between the two curves. Note that a high shipping direction ($A_s > 0$) is not necessarily a high noise direction ($A_N > 0$) since the angular noise distribution depends on the transmission

loss as well as the extent of the shipping in a given direction. Also note that there are always at least two steering angles for which an anisotropy is zero. In this report we say that directions for which the anisotropies are zero are isotropic directions, with the understanding that the noise or the shipping is isotropic if and only if all directions are isotropic directions.

To obtain the environmental parameters for a particular site of interest it is necessary to first determine the model components for that site, then compute the angular distributions from those components and finally compute the isotropic levels and the anisotropies for the array headings or beam steering angles of interest. To provide a basis for relating the results of this report to particular environments of interest we identify three representative cases: (1) anisotropic noise— isotropic shipping; (2) anisotropic shipping— isotropic noise; and (3) identical noise and shipping anisotropies. The first case occurs when the shipping is the same in all directions but either the transmission loss or the source level is a function of direction. The second case can occur when the shipping is close to the site in certain directions and distant from the site in other directions and the mean transmission loss is approximately that determined by cylindrical spreading. The third case occurs when the transmission loss is constant over the region of non-zero shipping. Conditions on the noise model components that result in these special cases are presented in Appendix C.

The numerical examples presented in this report are obtained for a fixed ideal sidelobe/mainlobe ratio, B_{s_0} , a fixed source-level distribution function, $F_{S(r,\theta)}$, and a fixed transmission loss function, $T(r,\theta)$. The value of the sidelobe/mainlobe ratio, -32.8 dB, is the value obtained for the broadside beam of a Hann-shaded array operating at the design frequency. Since B_{s_0} is fixed, the frequency and the steering angle are fixed, and hence a change in the directivity correspond to a change in the array length and a change in the anisotropies corresponds to a change in the array heading. The source-level distribution, which is specified in [1], is representative of the source-level of the noise radiated from merchant ships at moderate frequencies. The mean transmission loss $\bar{T}(r,\theta)$ is assumed to be independent of range and bearing over the region containing the shipping. As such it corresponds to the identical anisotropy case described above. The transmission loss fluctuations are described on a linear scale by an exponentially distributed random variable which is equivalent to assuming a multipath propagation model where the receptions on each of a number of paths are statistically independent with comparable levels. For this acoustics- fluctuation model and the source-level distribution of [1], the effect on the beam-noise fluctuations of the transmission loss fluctuations for a single transiting ship is less important than the effect of the variation in the source-level across the ensemble of ships.

3. Beam-noise distribution examples

In the introduction it was asserted that the extent of the beam-noise fluctuations is related to the extent to which ships are resolved in steering angle—small fluctuations occur for weakly resolved shipping; large fluctuations occur for highly resolved shipping. Furthermore, for highly resolved shipping, the low beam noise values are controlled by the sidelobe contributions; whereas, for weakly resolved shipping the beam-noise fluctuations are independent of the sidelobe contributions. In this section we present two examples of beam-noise distribution functions which support these assertions. The first example illustrates the effect of the extent of the shipping resolution using the directivity as the ship resolution parameter. The second example illustrates the effect of the sidelobe contributions using the sidelobe degradation as a parameter. Both examples are obtained for a fixed noise environment with an isotropic shipping level of unity ($D_0 = 1$ ship per degree bearing) and a beam that points in an isotropic noise direction ($A_N = 0$ dB) and an isotropic shipping direction ($A_S = 0$ dB.)

The distribution functions for the first example, shown in Fig. 3, were obtained for directivities ranging from 9 to 36 dB in 3-dB increments. The distributions for the smallest directivities and the largest directivities describe beam-noise fluctuations that occur in the manner described in the heuristic interpretation of Sect. 1. For the very low directivities (large beamwidths and hence weak shipping resolution), the beam-noise fluctuations occur over a comparatively small range of values (around 10 dB or less). The probability density for these fluctuations, which is the derivative of the distribution function, has the classical bell-shaped form that one would expect when the noise results from a number of ships located in the mainlobe sector. For the very large directivities (small beamwidths and hence high shipping resolution), the fluctuations occur over almost a 30 dB range. For these directivities the distribution shows a sharp increase over a small range of noise values in the vicinity of about -19 dB and then increases gradually towards its maximum value of 100% as the beam noise increases through the full range of values shown on the axis. The probability density corresponding to this distribution is large for noise values in a small interval about -19 dB, and small but non-zero for noise values to the right of this interval. Such a probability density describes beam-noise fluctuations that are concentrated in the small interval about -19 dB during most of the time but on rare occasions take on large positive values. In the heuristic discussion of Sect. 1, the low noise values were identified with the sidelobe contributions and the high noise values were identified with the mainlobe contribution.

The most striking feature of the distribution functions of Fig. 3 is that an increase in the extent of the noise fluctuations occurs primarily through an increase in the prevalence on the low noise values. That this is the case is evidenced by the fact

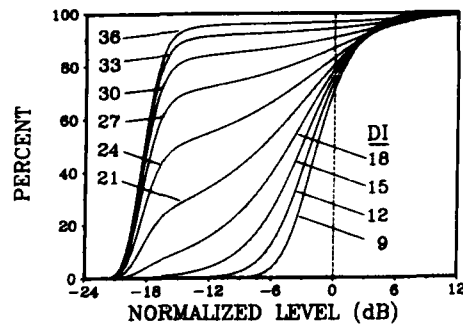


Fig. 3. Dependence of the beam-noise distribution function on the directivity for an isotropic shipping level of 1 ship/dg, 15 dB sidelobe degradation, and 0 dB shipping and noise anisotropies.

that an increase in the directivity results in a large increase in the distribution for low noise values but only a small decrease in the distribution for high noise values. For the low noise values (negative B) an increase in $F(B)$ corresponds to an increase in the probability that the noise is less than B , and hence to an increase in the percentage of time that low noise values are visible. For the high noise values (positive B), a decrease in $F(B)$ is equivalent to an increase in $1 - F(B)$, hence to an increase in the probability that the noise is greater than B , and hence to an increase in the percentage of time that high noise values are visible. As a numerical example, for $B = -12$ dB, an increase in the directivity from 15 to 21 dB increases the distribution by over 30% and hence results in a 30% increase in the percentage of time that noise values less than -12 dB are visible. On the other hand, for $B = +6$ dB, the same 6-dB increase in directivity reduces the distribution by less than 2% and hence results in less than a 2% increase in the percentage of time that noise values greater than $+6$ dB are visible.

A further inspection of Fig. 3 indicates that the effect of an increase in the directivity depends on whether that increase occurs for small directivities or large directivities. To describe this effect, we first introduce the notion of the beam-noise percentile. For a given percentage P , this quantity, which is denoted here by B_P , is that value of the beam noise satisfying

$$F(B_P) = P. \quad (9)$$

For P such that B_P is negative, $F(0) - P$ is the probability of observing noise values in the interval, $[B_P, 0]$, and hence B_P provides a measure of the range of low noise

values described by a particular distribution function. For the distributions of Fig. 3, B_P is negative for $P = 10\%$ and $F(0)$ is an increasing function of the directivity. Thus, for these distributions, a decrease in B_{10} corresponds to an increase in the range of the low noise values without a decrease in the percentage of time that those values are visible. Accordingly, B_{10} provides a measure of the dependence of the range of low noise values on the directivity. In this report we refer to B_{10} simply as the beam-noise percentile. The applicability of the beam-noise percentile in the more general setting will be discussed in the next section.

With this notion at hand the effect of an increase in the directivity on the low noise portion of the beam-noise distribution can be described as follows. For small directivities (less than 18 dB), an increase in the directivity results in a leftward shift in the lower tail of the distribution—the larger the directivity, the greater the shift. This leftward shift corresponds to a decrease in the beam-noise percentile and hence to an increase in the range of low noise values that are visible. For intermediate directivities (about 18 to 24 dB), an increase in the directivity results in a smaller leftward shift in the lower tail, hence a smaller decrease in the beam-noise percentile and hence a smaller increase in the range of low noise values. For these directivities, however, there is an increase in the level of the distribution in the vicinity of the tail. This increase corresponds to an increase in the probability of observing noise values comparable to the beam-noise percentile. Finally, for directivities larger than 24 dB there is essentially no leftward shift in the lower tail—only an increase in the level of the tail. For these directivities an increase in the directivity does not result in an increase in the range of low noise values that are visible—only in the percentage of time that the noise values at the lower extreme of this range are visible.

The preceding discussion suggests that there is a value of the beam noise, B_F , such that no matter how large the directivity noise values less B_F are observed only rarely. In this report we define B_F to be the limit of the beam-noise percentile as the directivity approaches infinity and refer to B_F as the 'noise floor'. By definition, the noise floor, which is about -20 dB for the distributions of Fig. 3, has the property that no matter how large the directivity noise values less than the noise floor occur less than 10% of the time. However, as seen in the distributions of Fig. 3, for sufficiently large directivities the distribution function is such that noise values slightly larger than the noise floor occur a high percentage of the time. We refer to these distributions as the noise-floor distributions and note that the percentage of time that the noise floor is 'visible' is approximately equal to the level of the noise-floor distribution in the vicinity of the noise floor. For the low directivities the distribution function is such that noise values comparable to the noise floor do not occur a significant percentage of the time. Except for the lowest directivities, these distributions exhibit a skew towards the low noise values that increases with increasing directivity. We refer to these distributions as the low-noise-skew distributions and note that for these distributions the noise floor is 'not visible'.

The distributions for the second example, shown in Figs. 4a and 4b, were obtained for

sidelobe degradations ranging from 0 to 25 dB in 5-dB increments. The distributions in Fig. 4a illustrate the effect of sidelobe degradation when the directivity (24 dB) is large enough for the distribution to have the noise-floor form. As seen in this figure, an increase in the sidelobe degradation results in a rightward shift in the lower tail of the distribution by essentially the same amount as the increase in the sidelobe degradation. This shift corresponds to an increase in the beam-noise percentile and hence to a reduction in the range of low noise values that are visible. Since the lower tail shows the same sharp increase for all sidelobe degradations, the increase in the sidelobe degradation does not alter the fact that the noise floor is visible, nor does it change the extent to which it is visible. Note that since there is no appreciable change in the upper tail of the distribution, the increase in the sidelobe degradation does not significantly change the percentage of time that high noise values are observed.

The distributions in Fig. 4b illustrate the effect of sidelobe degradation when the directivity (15 dB) is small enough for the distribution to have the low-noise skew form. In contrast to the distributions in Fig. 4a, these distributions show essentially no rightward shift in the lower tail as the sidelobe degradation increases from 0 to 15 dB, and only a small rightward shift as the sidelobe degradation increases from 15 to 25 dB. The increase in the beam-noise percentile and hence the decrease in the range of low noise values is only about 2 dB as the sidelobe degradation increases from 0 to 15 dB. Thus for directivities that are not large enough for the noise floor to be visible, an increase in the sidelobe degradation results in only a small reduction in the range of low noise values that are visible. As for the preceding case, there is no appreciable change in the upper tail of the distribution, so that in this case too, the increase in the sidelobe degradation does not significantly change the percentage of time that high noise values are visible.

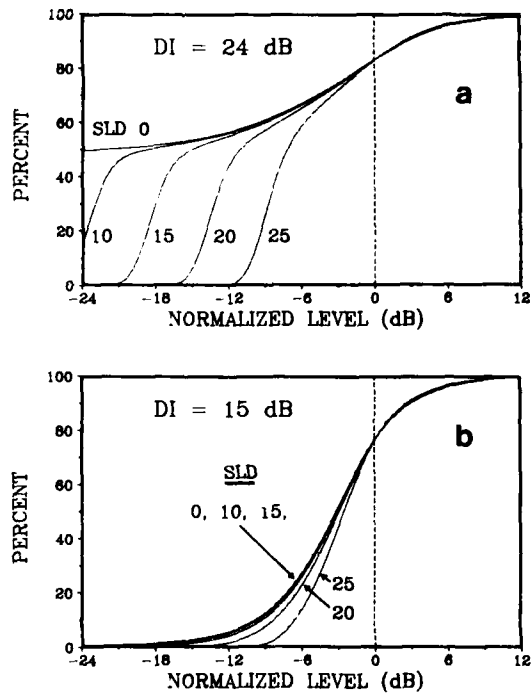


Fig. 4. Dependence of the beam-noise distribution function on the sidelobe degradation for an isotropic shipping level of 1 ship/dg and 0 dB shipping and noise anisotropies: (a) a directivity of 24 dB; (b) a directivity of 15 dB.

4. The beam-noise model approximations

In this section we present two approximations derived from the beam-noise model—the distribution approximation and the percentile approximation. The distribution approximation describes the beam-noise distribution in terms of two parameters which are related to the six physical parameters through simple equations. These equations provide conditions on the model parameters that result in approximately the same distribution function, and hence provide the basis for extending the results of Sect. 3 to the full set of model parameters. We then use the distribution approximation to specify conditions that identify the parameters that result in the noise-floor distributions and those that result in the low-noise-skewed distributions. These conditions, which involve only the ship resolution parameters—the directivity, the shipping anisotropy and the isotropic shipping level—are referred to as the resolution conditions in the spirit of the heuristic argument of Sect. 1. In addition, we use the distribution approximation to obtain a simple estimate for the percentage of time that the noise floor is visible in terms of the ship resolution parameters. The percentile approximation relates the beam-noise percentile to the sidelobe contribution parameters—the ideal sidelobe/mainlobe ratio, the sidelobe degradation and the noise anisotropy. As such, it provides an estimate of the noise floor when it is visible and an estimate of the range of low noise values that are visible when the noise floor is not visible.

The distribution approximation describes the beam-noise distribution as the sum of two terms—one that represents the noise contributions when there are ships in both the mainlobe sector and the sidelobe sector and one that represents the noise contributions when there are ships in only the sidelobe sector. The mainlobe/sidelobe term is the product of a probability $(1 - P_m)$ and a distribution function $F_{m,s}$, where $F_{m,s}$ is the distribution of the noise when there is at least one ship in the mainlobe sector and $1 - P_m$ is the probability that there is at least one ship in the mainlobe sector. The probability P_m , which is referred to here as the free-beam probability, is given by

$$P_m = \exp[-180 \times 10^{-R/10}], \quad (10)$$

where

$$R = DI - A_S - 10 \log[D_0]. \quad (11)$$

is referred to as the resolution parameter. The sidelobe term is the product, $P_m F_s(B - B_{s,d})$, where F_s is the distribution of the noise due only to the ships in the sidelobe sector and

$$B_{s,d} \doteq B_{s0} + SLD - A_N \quad (12)$$

is the sidelobe/mainlobe ratio for the degraded system with the beam pointing in an anisotropic noise direction. That the term $P_m F_s(B - B_{s,d})$ represents the sidelobe contributions follows from the fact that P_m is the probability that no ships lie in the

mainlobe sector and hence the probability that all ships lie in the sidelobe sector. The complete expression for the beam-noise distribution is

$$F(B) \doteq P_m F_s(B - B_{s_d}) + (1 - P_m) F_{m_s}(B; R, B_{s_d}). \quad (13)$$

In Eq. (13) we have ignored a weak dependence on both R and D_0 in the sidelobe distribution F_s . A discussion of the effects of this omission and the conditions under which the approximation is valid is presented in Appendix A. The exact equation for the sidelobe/mainlobe ratio B_{s_d} is given in Appendix B.

The conditions on the model parameters that lead to approximately the same distribution function follow immediately from the distribution approximation. According to the approximation, the distribution depends on the model parameters only through its dependence on the resolution R and the sidelobe/mainlobe ratio B_{s_d} , provided that the slight dependence of F_s on D_0 is ignored. Consequently, with this provision, the beam-noise distribution is approximately the same for all shipping resolution parameters that satisfy (11) for a constant R and all sidelobe contribution parameters that satisfy (12) for a constant B_{s_d} . In this report we refer to the conditions of Eqs. 11 and 12 as the equivalence conditions.

The equivalence conditions can be applied to the examples of Sect. 3 to obtain descriptions of the distribution function for other sets of model parameters. As an example of the procedure, consider the distributions of Fig. 3. These distributions were obtained for directivities that increase from 9 to 36 dB in 3-dB increments, a shipping anisotropy of 0 dB, an isotropic shipping level of one ship per degree, a 15-dB sidelobe degradation and a zero dB noise anisotropy. Thus, for these distributions, $B_{s_d} = B_{s_0} + 15$ dB and the resolution parameters are the same as the directivities. Consequently, these distributions can be relabeled using any sidelobe contribution parameters that result in the same value of B_{s_d} and any shipping resolution parameters that result in the same values of R . For example, the ten successive values of the directivity can be replaced by shipping anisotropies that decrease from 15 dB to -12 dB in 3-dB increments if the directivity is fixed at 24 dB and the isotropic shipping level remains at one ship per degree. Note that with this relabeling, the distributions of Fig. 3 indicate that the noise-floor distribution occurs for small shipping anisotropies and the low-noise skew distribution occurs for large shipping anisotropies.

The same procedure can be applied to the distributions of Figs. 4a and 4b to obtain alternative descriptions of the dependence of the distribution function on the sidelobe contribution parameters. For example, in both figures, the five successive values of the sidelobe degradation can be replaced by noise anisotropies that decrease from 0 to -25 dB in 5-dB increments if the sidelobe degradation is fixed at zero dB. With this relabeling the distributions of Fig. 4a indicate that for resolution parameters large enough to result in the noise-floor distribution, a decrease in

the noise anisotropy results in a corresponding increase in the noise floor. Similarly, the relabeled distributions of Fig. 4a indicate that for resolution parameters small enough to result in the low-noise skewed distribution, a decrease in the noise anisotropy results in at most a small increase in the beam-noise percentile.

Through the application of the equivalence conditions to the examples of Sect. 3, it is seen that the results of those examples can be generalized by simply replacing the directivity with the resolution parameter and the sidelobe degradation with the sidelobe/mainlobe ratio. The results can be summarized as follows. For sufficiently large values of the resolution parameter R , the distribution function has the noise-floor form characterized by the sharp rise in the lower tail of the distribution that occurs near the noise floor. For these resolutions, an increase in R increases the percentage of time that the noise floor is visible without altering its value; an increase in the sidelobe/mainlobe ratio B_{s_d} increases the value of the noise floor by a corresponding amount without altering the percentage of time that it is visible. For small values of R , where the noise floor is not visible, the distribution function has the low-noise-skewed form. The location of the lower tail of the distribution is specified by the beam-noise percentile B_{10} . For these resolutions, an increase in R results in a decrease in the beam-noise percentile and hence an increase in the range of low noise values that are visible; an increase in B_{s_d} has essentially no effect on either the beam-noise percentile or the distribution function.

The conditions that determine which form of the distribution function occurs follow from a consideration of the dependence of the distribution function on the beam-free probability and the sidelobe/mainlobe ratio. To describe this dependence, we have computed a beam-noise distribution using the exact model and plotted the result in Fig. 5. For this distribution P_m is about 50%, so that both terms in the distribution approximation are significant. Moreover, the sidelobe/mainlobe ratio B_{s_d} is a large negative number (about -25 dB), so that the sidelobe contribution term, $P_m F_s(B - B_{s_d})$ contributes to the distribution only for very low noise values. For these low noise values, the distribution shows a sharp increase over a small range of values. According to the approximation the form of this increase is determined by the sidelobe distribution $F_s(B)$; the level of the increase is determined by P_m ; and the noise value at which the increase occurs is determined by B_{s_d} . For the larger noise values, the distribution shows a gradual increase. According to the approximation, for this range of noise values the distribution function is approximately equal to $P_m + (1 - P_m)F_{m_s}(B; R, B_{s_d})$, since for these noise values the sidelobe contribution term is approximately equal to P_m . Thus for the larger noise values the form of the distribution is determined by the mainlobe/sidelobe distribution F_{m_s} .

It follows from the preceding discussion that the noise-floor distribution occurs only when P_m is sufficiently large and that when the noise floor is visible P_m provides an estimate of the extent to which it is visible. This is seen by noting that if P_m is large, the first term in (13) is significant and it is this term that gives rise to the sharp increase in the distribution that is present when the noise floor is visible.

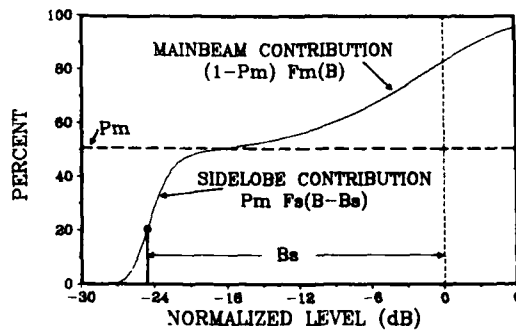


Fig. 5. The relationship between the beam-noise distribution function and the beam-free probability and the sidelobe/mainlobe ratio parameters.

Conversely, if P_m is small only the second term in (13) is significant. Consequently when P_m is small there is no sharp increase in the distribution at noise values comparable to the noise floor, and hence the noise floor is not visible. The beam-free probability determines the extent to which the noise floor is visible, since when P_m is large P_m is approximately equal to the level of the distribution in the vicinity of the noise floor and hence approximately equal to the percentage of the time that noise values comparable to the noise floor are visible. We note in passing that the sidelobe/mainlobe ratio provides a rough estimate of the noise floor, since this ratio determines the location of the sidelobe density on the noise axis and hence the noise values where the sharp increase in the distribution occur.

In this report we adopt the convention that the noise floor is visible whenever P_m exceeds 10% and not visible whenever P_m is less than 2%. When the noise floor is visible we say that the shipping is highly resolved. When it is not visible we say that the shipping is weakly resolved. The conditions that determine when the shipping is highly resolved and when it is weakly resolved are obtained by solving (10) for the two values of P_m and using (11) to express the results terms of the ship resolution parameters. These conditions, which we refer to as the resolution conditions, are given by

$$DI - A_s - 10 \log[D_0] > 18.9, \quad \text{for highly resolved shipping;} \quad (14a)$$

$$DI - A_s - 10 \log[D_0] < 16.6, \quad \text{for weakly resolved shipping.} \quad (14b)$$

According to this convention, the noise-floor distribution function occurs for highly

resolved shipping and the low-noise-skewed distribution occurs for weakly resolved shipping. That this is the case is evidenced by the distributions of Fig. 3 where the shipping is highly resolved for directivities greater than 18.9 dB and weakly resolved for directivities less than 16.6 dB.

According to the resolution conditions, highly resolved shipping (noise floor visible) occurs for systems with high directivity, operating areas with light shipping, or beams that point in low shipping directions. Whenever these conditions are satisfied, a number of individual ships will be resolved in steering angle a high percentage of the time. Conversely, weakly resolved shipping (noise floor not visible) occurs for systems with low directivity, operating areas with heavy shipping, or beams that point in high shipping directions. When these conditions are satisfied, individual ships will be resolved in steering angle only rarely. Note that only a 2.3-dB increase in the shipping resolution is required to transition from weakly resolved to highly resolved shipping. This can occur for either a 2.3-dB increase in the directivity, a 2.3 dB reduction in the shipping anisotropy or a 58% reduction in the isotropic shipping level.

When the shipping is highly resolved, the free-beam probability is approximately equal to the percentage of time that the noise floor is visible. This probability is determined from the ship resolution parameters by Eqs. 10 and 11. According to these equations, once the shipping becomes highly resolved, any change in the shipping resolution parameters that results in an increase of 6 dB in R , increases the percentage of time that the noise floor is visible from 10% to 50%. Moreover, any change that results in an additional increase of 6 dB in R , increases this percentage from 50% to 82%. For larger values of R , the percentage of time that the noise floor is visible increases gradually with R towards its limiting value of 100%.

The percentile approximation provides two expressions for the beam-noise percentile: one for highly-resolved shipping and one for weakly-resolved shipping. The approximation for highly-resolved shipping is obtained from the distribution approximation by noting that for highly resolved shipping, the maximum value of the sidelobe contribution term $P_m F_s(B - B_{sd})$ exceeds 10%, since P_m exceeds 10%. Consequently, the beam-noise percentile is determined by the condition $P_m F_s(B_{10} - B_{sd}) = 10\%$ (see Eq. (9)). It follows from this condition that the beam-noise percentile for any set of sidelobe contribution parameters can be expressed in terms of that obtained for some set of reference parameters. In this report we take the reference parameters to be those corresponding to the ideal system with zero sidelobe degradation and zero noise anisotropy and denote the reference percentile by B_{10_0} . The percentile approximation for highly resolved shipping is then given by

$$B_{10} \doteq B_{10_0} + \text{SLD} - A_N. \quad (15a)$$

An analogous approximation for the noise floor is obtained by taking the limit of

both sides of (15a) as the directivity approaches infinity. The result is

$$B_F \doteq B_{F_0} + \text{SLD} - A_N, \quad (15b)$$

where B_{F_0} is the noise floor for the reference parameters. Clearly, the approximation of Eq. (15a) will hold for any percentage P provided that $P > P_m$. An example of the relationship between B_P and B_{F_0} for $P = 26\%$ is shown in Fig. 6a.

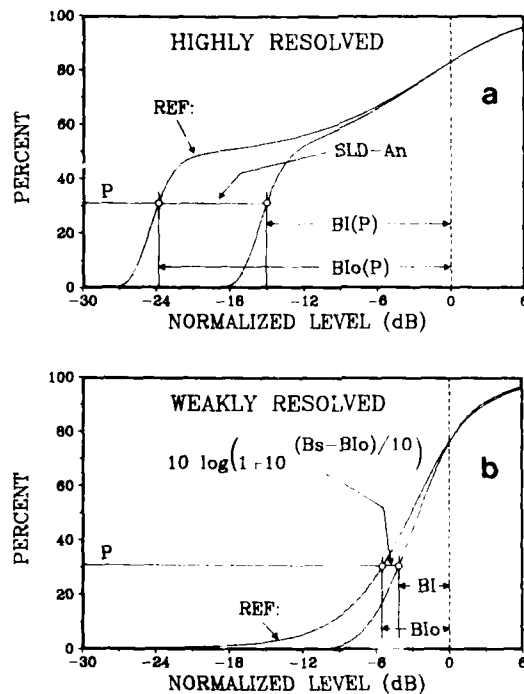


Fig. 6. Beam-noise percentile approximation: (a) highly resolved shipping and (b) weakly resolved shipping.

When the shipping is weakly resolved, the beam-noise distribution is approximately equal to the mainlobe distribution. For this case it is shown in [6] that for any

percentage P the beam-noise percentile for arbitrary sidelobe degradations and noise anisotropies is related to B_{P_0} by

$$B_P \doteq B_{P_0} + 10 \log[1 + 10^{(B_{sd} - B_{P_0})/10}]. \quad (16)$$

An example of the relationship between B_P and B_{P_0} for $P = 26\%$ is shown in Fig. 6b.

The percentile approximations indicate that for both highly-resolved and weakly-resolved shipping the beam-noise percentile is an increasing function of the sidelobe degradation and a decreasing function of the noise anisotropy. For highly resolved shipping, both the beam-noise percentile and the noise floor increase linearly with the sidelobe degradation and decrease linearly with the noise anisotropy. An example of the effect of an increase in the sidelobe degradation was seen in the beam-noise distributions of Fig. 4a. For weakly resolved shipping, the approximation indicates that the beam-noise percentile is weakly dependent on the sidelobe degradation and the noise anisotropy. For the particular example shown in Fig. 6b, which was obtained for a 25-dB sidelobe degradation in an isotropic noise direction, the beam-noise percentile increases by only about 2 dB relative to the reference beam-noise percentile. This lack of sensitivity is consistent with that observed in the distribution functions of Fig. 4b.

We conclude this section with two examples of the beam-noise percentile. These examples are intended to both illustrate the principles presented in this section and to provide numerical examples for use in the following section. The percentile curves for the first example, shown in Fig. 7, describe the beam-noise percentile as a function of the directivity for three values of the sidelobe degradation: 0, 10, and 20 dB. The isotropic shipping level is two ships per degree and the beam points in an isotropic shipping direction and an isotropic noise direction. For these parameters, the shipping is weakly resolved when the directivity is less than 19.6 dB and highly resolved when the directivity exceeds 21.9 dB. The percentile curve for 0-dB sidelobe degradation is a reference percentile curve.

The percentile curves of Fig. 7 each show a gradual decrease as the directivity increases up to the weakly-resolved shipping bound (19.6 dB), followed by a large decrease as the directivity increases by 2.3 dB to the highly-resolved shipping bound (21.9 dB), followed by an abrupt decrease to the noise floor as the directivity increases a few decibels beyond the highly-resolved shipping bound. For weakly resolved shipping, the distribution has the low-noise skewed form and, for highly resolved shipping, the distribution has the noise-floor form. Thus these curves indicate that the transition from the low-noise-skewed distribution to the noise-floor distribution occurs through a large decrease in the beam-noise percentile. Furthermore, once the shipping becomes highly resolved, only a small increase in the resolution is necessary to reduce the beam-noise percentile to the noise floor. This behavior is consistent with the distribution functions of Fig. 3.

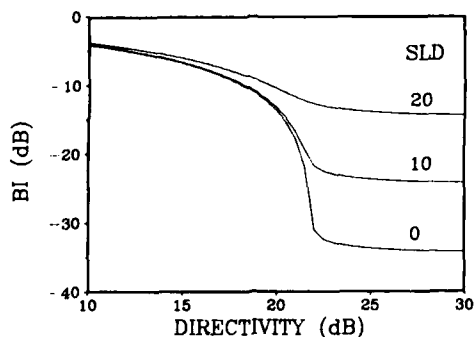


Fig. 7. Dependence of the 10% beam-noise percentile on the directivity for a shipping strength of 2 ships/dg, 0 dB shipping and noise anisotropies, and selected values of the sidelobe degradation (SLD).

Of the three percentile curves shown in Fig. 7, the beam-noise percentile for the reference case (0 dB sidelobe degradation; 0 dB noise anisotropy) has the lowest values. This percentile decreases by about 8 dB as the directivity increases from 10 to 19.6 dB, by about 18 dB as the directivity increases from 19.6 to 21.9 dB, and by less than 4 dB as the directivity increases from 21.9 to 30 dB. The other percentile curves lie above the reference percentile by the amount predicted by the percentile approximations. For the weakly resolved shipping directivities, the 10-dB percentile curve is essentially equal to the reference percentile curve and the 20-dB percentile curve is less than 2 dB larger than the reference percentile curve; for the highly resolved shipping directivities, the 10-dB and the 20-dB percentile curves lie above the reference percentile curve by an amount that is approximately equal to the sidelobe degradation.

The percentile curves for the second example, shown in Fig. 8, describe the beam-noise percentile as a function of the directivity for five values of the isotropic shipping level. The sidelobe degradation is zero and the beam again points in an isotropic shipping direction and an isotropic noise direction. For these parameters, the minimum directivity required for highly resolved shipping increases in 3-dB increments from 16 to 28 dB as the shipping strength increases from 0.5 to 8 ships per degree in powers of two. The percentile curve for 2 ships per degree is the same as the reference percentile curve of Fig. 7.

As seen in Fig. 8, the five percentile curves are essentially translations of one another with the extent of the translation determined by the isotropic shipping levels, i.e. the

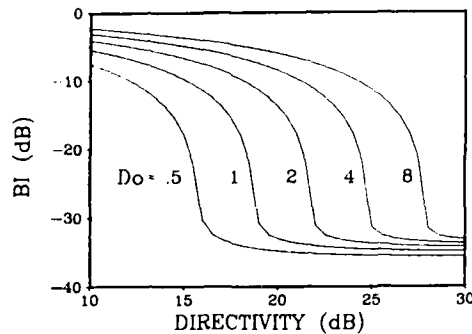


Fig. 8. Dependence of the 10% beam-noise percentile on the directivity for 0-dB sidelobe degradation, 0 dB shipping and noise anisotropies and selected values of the shipping strength (D_0).

curve obtained by doubling the shipping strength is shifted to the right by 3 dB. That this is the case is consistent with the distribution approximation since a doubling of the isotropic shipping level results in the same value of R only if the directivity is reduced by 3 dB. The single exception occurs for the noise floor portion of the percentile curves where the noise floor for the larger isotropic shipping levels is slightly larger than the noise floor for the smaller shipping levels. This discrepancy results from the slight dependence of the sidelobe distribution F_s on the isotropic shipping level (see Appendix A). Finally, note that for each percentile curve, the large decrease in the percentile occurs over the range of directivities predicted by the resolution conditions.

5. Examples

In the preceding section it was seen that the beam-noise distribution function is largely determined by the resolution parameter R and the sidelobe/mainlobe ratio B_{s_d} . These parameters are related to the six basic model parameters by Eqs. 11 and 12; the model parameters themselves are related to the components of the noise model through the definitions of Sect. 2. Accordingly, the results of the preceding section can be used to determine the basic characteristics of the distribution function for a number of problems of interest simply by expressing those problems in terms of the model parameters.

In this section, we present a number of examples that illustrate both the procedure and the nature of the results. The first three examples are concerned with the dependence of the distribution function on the array heading for a fixed system at a fixed site in one of the three canonical environments identified in Sect. 2. In these examples we limit the discussion to the effect of changes in the array heading with the understanding that the functional dependence on the array heading can only be determined from that of the shipping and noise anisotropies themselves. For the first two environments, anisotropic noise—*isotropic shipping* and *anisotropic shipping—*isotropic noise**, the effect of the array heading can be inferred immediately from the results of Sect. 4, since a change in the array heading affects only one of the two anisotropies and hence only one of the two parameters R and B_{s_d} . For these environments, numerical illustrations are obtained by applying the equivalence conditions to examples presented earlier. For the third environment, identical shipping and noise anisotropies, a change in the array heading affects both anisotropies and hence both R and B_{s_d} . For this environment, we illustrate the dependence through a numerical example of the beam-noise percentile computed as a function of the common anisotropy. In two final examples we briefly describe the dependence of the distribution function on the array length and the sidelobe degradation.

For the *anisotropic noise—*isotropic shipping** environment, the shipping anisotropy is identically zero and hence a change in the array heading results only in a change in the noise anisotropy. Consequently, the sidelobe/mainlobe ratio is a function of the array heading and the resolution parameter is independent of the array heading. There are two cases depending on whether the directivity and the *isotropic shipping* level are such that shipping is weakly resolved or highly resolved. If the shipping is weakly resolved, the distribution function has the low-noise-skewed form for all array headings and large variations in the noise anisotropy can occur without a significant change in the distribution function. On the other hand, if the shipping is highly resolved the distribution function has the noise-floor form and any change in the noise anisotropy results in an equal but opposite change in the value of the noise floor, i.e. array headings that place the beam in a high noise direction result in a low

SACLANTCEN SR-116

noise floor and vice versa. However, since the resolution parameter is independent of the array heading the level of the lower tail of the distribution is independent of the array heading, and hence, the percentage of time that the noise floor is visible is independent of the array heading. Thus, for this environment the distribution function depends on the array heading only when the shipping is highly resolved and then only through the value of the noise floor.

Numerical examples of the dependence of the distribution function on the noise anisotropy are obtained by relabeling Figs. 4a and 4b as described in Sect. 4. An example of the dependence of the beam-noise percentile is obtained from Fig. 7 by replacing the sidelobe degradations by noise anisotropies that decrease from 0 dB to -20 dB in 10-dB increments.

For the anisotropic shipping—*isotropic noise environment*, the noise anisotropy is identically zero and hence a change in the array heading results only in a change in the shipping anisotropy. Consequently the resolution parameter is a function of the array heading, and the sidelobe/mainlobe ratio is independent of array heading. For this environment, any change in the array heading that results in a change in the shipping anisotropy results in a change in the distribution function. For array headings such that the shipping is weakly resolved, the distribution function has the low-noise-skewed form and the beam-noise percentile, which describes the lower tail of that distribution, increases or decreases gradually with the shipping anisotropy. For array headings such that the shipping is highly resolved, the distribution has the noise floor form and the level of the lower tail (which determines the percentage of the time that the noise floor is visible) increases or decreases with the shipping anisotropy according to the free-beam probability equation. The value of the noise floor itself is independent of the array heading since the noise anisotropy is independent of the array heading. Finally, if the change in the array heading results in a transition from weakly-resolved to highly-resolved shipping, which occurs for a 2.3-dB decrease in the shipping anisotropy, there is a large decrease in the beam-noise percentile as the distribution changes from the low-noise-skewed form to the noise-floor form.

A numerical example of the dependence of the distribution function on the shipping anisotropy is obtained by relabeling Fig. 3 as described in Sect. 4. An example of the dependence of the beam-noise percentile on the shipping anisotropy can be obtained by relabeling the percentile curves of Fig. 8. This is done for a shipping strength of one ship per degree, by replacing the directivity axis with a shipping anisotropy axis that starts at +10 dB and finishes at -10 dB and by replacing the shipping strengths, 0.5, 1.0, 2.0, 4.0, and 8.0, with the directivities, 23, 20, 17, 14 and 11 dB.

For the third environment, identical shipping and noise anisotropies, the two anisotropies increase or decrease together as the array heading changes. Consequently both the sidelobe/mainlobe ratio and the resolution parameter are functions of the array heading. The dependence of the beam-noise percentile on the common anisotropy is described by the percentile curves of Fig. 9. The negative values of the

anisotropy correspond to low-noise and low-shipping directions; the positive values correspond to high-noise and high-shipping directions. The three curves shown are obtained for a shipping strength of 2 ships per degree, a sidelobe degradation of 15 dB and directivities of 15, 20 and 25 dB. For these directivities the maximum shipping anisotropies for which the shipping is highly resolved are about 3, -2 and -7 dB respectively; the minimum shipping anisotropies for which the shipping is weakly resolved are 2.3 dB higher.

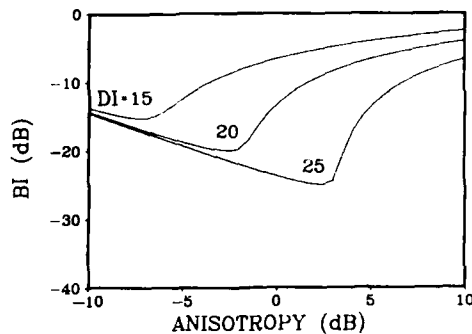


Fig. 9. Dependence of the 10% beam-noise percentile on the anisotropy for a shipping strength of 2 ships/dg, a sidelobe degradation of 10 dB and selected values of the directivity (DI).

An inspection of the percentile curves of Fig. 9 shows that for each directivity there is an 'optimum' anisotropy for which the beam-noise percentile achieves a minimum value. This optimum anisotropy is approximately equal to the highly-resolved shipping bound as seen through the comparison of the value on the plot with the bound obtained from the resolution conditions. That the beam-noise percentile must increase for anisotropies to either side of the highly resolved shipping bound can be seen as follows. For anisotropies less than the optimum anisotropy, the shipping is highly resolved and hence the beam-noise percentile is independent of the shipping anisotropy and it is a linearly decreasing function of the noise anisotropy. Thus, since the common anisotropy describes both the noise anisotropy and the shipping anisotropy, the beam-noise percentile must increase linearly as the common anisotropy decreases below the optimum anisotropy. On the other hand, for anisotropies that are about 2.3 dB larger than the optimum anisotropy the shipping is weakly resolved. For these anisotropies, the beam-noise percentile is independent of the noise anisotropy and it is an increasing function of the shipping anisotropy.

Consequently, the beam-noise percentile must increase as the common anisotropy increases above the optimum anisotropy.

According to the preceding example, the effect of changes in the array heading on the distribution function will depend on whether the beam points in a direction where the common anisotropy exceeds the optimum anisotropy or a direction where the common anisotropy is less than the optimum anisotropy. For array headings such that the common anisotropy is about 2.3 dB larger than the optimum anisotropy, the shipping is weakly resolved and hence the distribution function has the low-noise-skewed form. For these anisotropies an increase in the common anisotropy due to a change in the array heading results in an increase in the beam-noise percentile, and hence a decrease in the range of low noise values. This dependence is the same as that for the anisotropic noise—*isotropic shipping environment* when the shipping is weakly resolved. On the other hand, for array headings such that the anisotropy is less than the optimum anisotropy, the shipping is highly resolved and the distribution has the noise floor form. For these anisotropies, a decrease in the common anisotropy due to a change in the array heading results in an increase in the value of the noise floor and a decrease in the level of the distribution near the noise floor. The noise floor increases because the noise anisotropy decreases; the level of the distribution decreases because the shipping anisotropy decreases. This dependence differs from that of the other environments in that both the value of the noise floor and the percentage of time that it is visible depend on the array heading.

The dependence of the distribution on the sidelobe degradation and the array length for a fixed environment is analogous to that described for the first two environments. If the sidelobe degradation is treated as an independent parameter, the dependence is the same as that obtained for the anisotropic noise—*isotropic shipping environment* except that low/high noise anisotropies correspond to high/low sidelobe degradations. Thus if the shipping is weakly resolved the distribution function has the low-noise-skewed form and large sidelobe degradations can be tolerated without a significant change in the distribution function. Conversely, if the shipping is highly resolved the distribution function has the noise-floor form and any change in the sidelobe degradation results in a corresponding change in the noise floor, but not in the percentage of time that it is visible. Numerical examples of the dependence on the sidelobe degradation are found in Figs. 4a, 4b and 7. If the sidelobe degradation is to be described in terms of the errors that produce that degradation, then Eq. (B.7c) of Appendix B can be used to relate the sidelobe degradation parameter to the parameter that describes those errors.

The dependence of the distribution on the array length is qualitatively the same as that obtained for the anisotropic shipping—*isotropic noise environment* with large array lengths corresponding to low shipping anisotropies. This is seen by noting that the array length affects only the directivity, so that the resolution parameter remains unchanged if the negative of the shipping anisotropy is replaced by the directivity. It follows that for array lengths where the shipping is weakly resolved the distribution

has the low-noise-skewed form, so that an increase in the array length results in a gradual decrease in the beam-noise percentile and hence a gradual increase in the range of low noise values that are visible. For array lengths such that the shipping is highly resolved the distribution has the noise-floor form, so that an increase in the array length results in an increase in the percentage of time that the noise floor is visible without a decrease in the noise floor itself. In order to transition from weakly resolved to highly resolved shipping, the array length must be increased by 58%. The dependence on array length can be seen in the plots of Figs. 3, 8 and 9 simply by expressing the directivity in terms of the array length.

Finally, it is noted that the numerical examples of the distribution function $F(B)$ presented in this report are easily converted to examples of the distribution function for the total beam noise $F_T(B)$ by using the relationship $F_T(B) = F(B - B_m)$, where B_m is given by Eq. (B.17). As noted in Appendix B, for most situations, B_m depends only on the directivity and the noise anisotropy. Thus for those examples that do not involve these parameters the distribution functions for the total beam noise are obtained by simply relabeling the beam-noise axis. For those examples that do involve these parameters, each distribution must be shifted by an amount determined by the value of the parameter. Examples of the beam-noise percentile for the total beam noise are obtained from the examples of the beam-noise percentile for the fluctuating component by adding the mean beam noise to each percentile curve.

6. Summary and conclusions

This report has described properties of the beam-noise distribution function determined from a Poisson shipping noise model that describes the horizontal array system and the noise environment in terms of six parameters. The properties are obtained using approximations derived from that model to extend the characteristics observed in examples of the distribution function for specific parameters to the full parameter set. According to these approximations the dependence of the distribution function on the model parameters can be expressed in terms of only two parameters—a resolution parameter R and the sidelobe/mainlobe ratio $B_{s,l}$. The resolution parameter, which is a linear function of the directivity, the isotropic shipping level and the shipping anisotropy, provides a measure of the extent to which individual ships are resolved in steering angle. The sidelobe/mainlobe ratio, which is a linear function of the ideal sidelobe/mainlobe ratio, the sidelobe degradation and the noise anisotropy, is a direct measure of the relative contribution of the noise power in the sidelobe sector to that in the mainlobe sector.

The report has shown that the distribution function takes two different forms—one that results when the shipping is weakly resolved and one that results when the shipping is highly resolved. For weakly resolved shipping the distribution describes comparatively small beam-noise fluctuations. The shape of this distribution corresponds to that of the classical bell-shaped probability density with a skew towards the low noise values. For these distributions the beam-noise percentile B_{10} specifies the location of the lower tail and hence the range of low noise values that are visible. For highly resolved shipping the distribution describes fluctuations that range from very low values to very high values. The lower tail of these distributions exhibits a sharp rise at the low noise values indicating that these values occur a significant percentage of the time. The lowest noise values that are visible are identified by the noise floor, which was defined as the limit of the beam-noise percentile as the resolution parameter approaches infinity.

A formal definition of weakly resolved and highly resolved shipping is provided by the resolution conditions (Eq. (14)). These conditions, which depend only on the shipping resolution parameters, indicate that merely a 2.3-dB increase in the directivity, or a 2.3-dB increase in the shipping anisotropy, or a 58% reduction in the isotropic shipping level is required to transition from weakly resolved to highly resolved shipping. For highly resolved shipping the free-beam probability (Eq. (11)) provides an estimate of the level of the lower tail of the distribution, and hence an estimate of the percentage of time that the noise floor is visible. The percentile approximations (Eqs. (15) and (16)) provide estimates for the beam-noise percentile for both weakly resolved and highly resolved shipping in terms of the sidelobe degradation,

the noise anisotropy and the beam-noise percentile for zero sidelobe degradation and zero noise anisotropy.

The noise model approximations were used to obtain a description of the dependence of the beam-noise distribution on the full set of model parameters. This dependence is summarized as follows:

- For weakly resolved shipping, where the distribution has the low-noise-skewed form, an increase in the resolution results in an increase in the beam-noise percentile and hence an increase in the range of low noise values that are visible. A change in either the sidelobe degradation or the noise anisotropy has essentially no effect on either the beam-noise percentile or the distribution function.
- For highly resolved shipping, where the distribution has the noise-floor form, the beam-noise percentile is approximately equal to the noise floor. An increase in the resolution results in an increase in the percentage of time that low noise values are visible without increasing the range of those low noise values. For these distributions, an increase in either the sidelobe degradation or a decrease in the noise anisotropy results in a corresponding increase in the noise floor.
- The 2.3-dB increase in the resolution required to transition from weakly resolved to highly resolved shipping results in a large decrease in the beam-noise percentile. This decrease can exceed 18 dB for a system with zero sidelobe degradation and a beam pointing in a high noise direction.
- For both weakly resolved and highly resolved shipping, a large increase in the resolution results in only slight decrease in the level of the upper tail of the distribution and hence only a slight increase in the percentage of time that high noise values are visible. The upper tail of the distribution is essentially independent of the sidelobe degradation and the noise anisotropy.

Finally, we described the dependence of the distribution function on the array heading for three canonical noise environments and briefly summarized its dependence on the array length and the sidelobe degradation.

References

- [1] HEITMEYER, R. A model for the beam-noise fluctuations for a horizontal array operating in a ship-induced noise field, SACLANTCEN Report, in preparation.
- [2] GOLDMAN, J. unpublished work, Whippany, N.J., Bell Telephone Laboratories.
- [3] MOLL, M., ZESKIND, R.M. and SCOTT, W.L. An algorithm for beam-noise prediction, BBN 3653. Arlington, VA, Bolt, Beranek Newman Inc., 1979. [AD A0 76615]
- [4] HEITMEYER, R., SCRIMGER, P. and BOULON, P. A probabilistic model for shipping traffic with applications to the Mediterranean, SACLANTCEN Report, in preparation.
- [5] HEITMEYER, R., DAVIS, L. and YEN, N. Implications of noise source resolution on detection performance for horizontal directional systems operating in ship-induced noise fields, Report 8863. Washington DC, Naval Research Laboratory, 1985.

SACLANTCEN SR-116

- 32 -

intentionally blank page

Appendix A

Noise model equations

The basic assumptions of the model lead to an expression for the characteristic function of the beam-noise, $\phi(u)$. This function is defined by $\phi(u) = E[\exp(iub_T)]$ where $E[\cdot]$ is the expected value operator and $b_T = 10^{B_T/10}$ is the total beam noise expressed in a linear scale. The beam-noise distribution function is obtained using the fact that the probability density is the Fourier transform of ϕ . Under the assumptions of the model it is shown in [1] that the characteristic function is given by

$$\phi(u) = \exp \left[\int_{\mathbf{R}} D(r, \theta) [\phi_P(u; r, \theta) - 1] dA(r, \theta) \right], \quad (\text{A.1a})$$

where

$$\phi_P(u; r, \theta) = E(\exp[iuS(r, \theta)T(r, \theta)B_A(\theta, \theta_s)]) \quad (\text{A.1b})$$

is the characteristic function for the noise contribution from a single ship at range r and bearing θ ; $dA(r, \theta)$ is the area element on a spherical earth; and \mathbf{R} is the region containing the ships. Expressions for the moments of the beam noise are obtained as a corollary to the model. The first moment, the mean beam noise, is given by

$$\bar{b}_T = \int_0^{2\pi} n(\theta) B_A(\theta) d\theta, \quad (\text{A.2})$$

where $n(\theta)$ is the angular noise distribution of Eq. (5). The expression for the angular shipping distribution, Eq. (6), follows immediately from the definition of the spatial shipping density.

For the two-valued beam pattern, it is shown in [1] that the distribution function depends on three parameters, the sidelobe/mainlobe ratio $B_{s,l}$, the mean number of ships in the mainlobe sector M_m , and the mean number of ships in the sidelobe sector M_s . The parameters M_m and M_s are obtained from the folded angular shipping distribution by

$$M_m = \int_{\mathbf{BW}_0} d_F(\theta', \theta_s) d\theta', \quad (\text{A.3a})$$

$$M_s = \int_{\mathbf{BW}_0} d_F(\theta', \theta_s) d\theta'. \quad (\text{A.3b})$$

Expressions for $B_{s,l}$, M_m and M_s in terms of the physical parameters are presented in Appendix B.

The exact expression for the distribution function is the sum of four terms. These terms describe the noise contribution under four conditions: no ships in either the sidelobe sector or the mainlobe sector; ships in the mainlobe sector but not in the

sidelobe sector; ships in the sidelobe sector but not in the mainlobe sector; and ships in both the sidelobe sector and the mainlobe sector. The distribution approximation is obtained under two assumptions. First, it is assumed that the mean number of ships in the sidelobe sector M_s is large enough that the probability that there are no ships in the sidelobe sector, $P_s = \exp\{-M_s\}$, is negligible. This assumption will be satisfied except in areas of extremely light shipping, e.g. if $M_s > 5$, $P_s < 0.01$ and the approximation is acceptable. Environments where this assumption is not satisfied are not of practical importance since the noise from other sources will dominate the ship-induced noise component. Under this assumption, the first two terms in the sum can be neglected. Secondly, it is assumed that the three parameters satisfy

$$B_{s_d} < -10 + 5 \log(M_s/M_m). \quad (A.4)$$

This condition states that the relative noise contribution from ships in the sidelobe sector cannot be large in comparison with the relative number of ships in the sidelobe sector. This condition will be satisfied for almost all noise environments and all systems except those with extreme sidelobe degradation. For example, with a conservative value of $M_s/M_m = 10$ and B_{s_d} given by (12) with $B_{s_0} = -32.8$ dB, the condition (A.4) is satisfied provided that

$$SLD - A_N < 27.8 \text{ dB.}$$

Under this assumption, the last term in the sum can be considerably simplified. The third term in the sum, which represents the sidelobe contributions, is retained in the approximation. The distribution approximation is expressed in terms of the three parameters M_m , M_s and B_{s_d} and the distributions F_s and F_{m_s} by

$$F(B; M_m, M_s, B_{s_d}) \doteq P_m F_s(B - B_{s_d}; M_s) + (1 - P_m) F_{m_s}(B; M_m, B_{s_d}) \quad (A.5)$$

where

$$P_m = \exp\{-M_m\} \quad (A.6)$$

is the probability of no ships in the mainlobe sector and

$$F_{m_s}(B; M_m, B_{s_d}) = \begin{cases} F_m(B + g(B, B_{s_d}); M_m), & \text{if } B > B_{s_d} - 10 \log[1 + 10^{B_{s_d}/10}]; \\ 0, & \text{otherwise.} \end{cases} \quad (A.7a)$$

where

$$g(B, B_{s_d}) = 10 \log\{(1 + 10^{B_{s_d}/10})(1 - 10^{B/10})\} \quad (A.7b)$$

and $F_m(\cdot; M_m)$ is the distribution function for the noise due only to ships in the mainlobe sector, given that there is at least one ship. The derivation on this approximation is contained in [1].

The distribution approximation of Sect. 2, which depends on only two parameters, R and B_{s_d} , is obtained from the approximation of (A.5)-(A.7) and the expression for M_m , M_s and B_{s_d} derived in Appendix B. The approximate expression for B_{s_d} of Eq. (12) is obtained by neglecting a term in the exact expression, Eq. (B.13a). The parameter M_m is expressed solely in terms of R by neglecting a weak dependence on the ideal sidelobe/mainlobe ratio B_{s_0} and the channel error parameter s_c (see Eq. (B.21)). The parameter M_s , which controls the shape of the sidelobe distribution F_s , depends on both R and D_0 (see Eq. (B.23)). However in [5] it is shown through numerical examples that for typical values of M_s large changes in M_s result in only small changes in the shape of F_s . Thus, by dropping the dependence of the sidelobe distribution on M_s , and hence on D_0 and R , we are ignoring these small changes in the shape of F_s .

Appendix B

Derivations of the model parameters

The two-valued beam pattern is specified by two parameters: the beamwidth BW and the sidelobe level S_d . As stated in Appendix A, the beam-noise distribution for the two-valued beam pattern depends on three parameters: the sidelobe/mainlobe ratio B_{s_d} , the mean number of ships in the mainlobe sector M_m , and the mean number of ships in the sidelobe sector M_s . The fluctuations in the total beam noise are determined from the mean beam noise B_m . In this Appendix we derive the expressions for these parameters in terms of the physical parameters defined in Sect. 2. In these derivations, the noise powers and the sidelobe levels are expressed in a linear power scale. To avoid confusion between the decibel quantities used in Sect. 2 and the linear quantities used in the derivations we use a lower-case symbol for the linear quantities.

B.1. DERIVATION OF BW AND S_d

The two-valued beam pattern parameters are obtained under the assumption that the degradation in the system results from statistically independent, identically distributed, channel-to-channel errors. It follows from this assumption that the mean value of the actual beam pattern can be written in terms of the ideal beam pattern according to

$$B_{A_d}(\theta, \theta_s) = (1 - s_e)B_{A_0}(\theta, \theta_s) + s_e, \quad (\text{B.1})$$

where s_e is a constant determined by the common probability density for the channel errors. The parameters BW and S_d are determined such that the mean beam noise and the sidelobe/mainlobe ratio for the actual beam pattern and the two-valued approximation are identical for an isotropic noise field. Since the maximum of both beam patterns is unity the mean beam noise requirement will be satisfied if the integrals of the actual beam pattern and the approximation are equal (see Eq. (A.2)). By using the two-valued approximation of Eq. (1) along with the actual beam pattern of Eq. (B.1) and Eq. (2b) in the main text, it is seen that the mean beam noise requirement will be satisfied if

$$N_0[s_d(\pi - \text{BW}) + \text{BW}] = \bar{b}_T, \quad (\text{B.2a})$$

where

$$\bar{b}_T = N_0[(1 - s_e)\text{BW}_0 + s_e\pi] \quad (\text{B.2b})$$

is the mean value of the total beam noise and N_0 is the isotropic noise level. The condition for identical sidelobe/mainlobe ratios is obtained by substituting the beam patterns of Eq. (1) and Eq. (B.1) into the definition on the sidelobe/mainlobe ratio

(Eq. (3) in the main text), equating the results, and using the fact that

$$\int_{\text{BW}_0} B_{A_0}(\theta', \theta_s) d\theta = \text{BW}_0 / (1 + b_{s_0})$$

and

$$\int_{\text{BW}_0} B_{A_0}(\theta', \theta_s) d\theta = \text{BW}_0 b_{s_0} / (1 + b_{s_0})$$

to simplify the expression for the sidelobe/mainlobe ratio for the actual beam pattern. The result is

$$s_d(\pi - \text{BW}) / \text{BW} = b_{s_d}, \quad (\text{B.3a})$$

where

$$b_{s_d} = ((1 - s_e)b_{s_0} + s_e(10^{D_1/10} - 1)(1 + b_{s_0})) / (1 + s_e b_{s_0}) \quad (\text{B.3b})$$

is the sidelobe/mainlobe ratio for the actual beam pattern. Equations (B.2a) and (B.3a) can be solved to obtain BW and s_d in terms of $\bar{b}_T(s_e)$, $b_{s_d}(s_e)$ and the ratio π / BW . The results are

$$\text{BW} = \bar{b}_T / (1 + b_{s_d}), \quad (\text{B.4})$$

and

$$s_d = b_{s_d} / ((\pi / \text{BW}) - 1), \quad (\text{B.5a})$$

where

$$\pi / \text{BW} = \pi(1 + b_{s_d}) / \bar{b}_T. \quad (\text{B.5b})$$

The desired results are obtained by substituting Eqs. (B.2b) and (B.3b) into Eqs. (B.4) and (B.5) and rearranging. The resulting beamwidth is

$$\text{BW} = \text{BW}_0(1 + s_e 10^{B_{s_0}/10}) / (1 + 10^{B_{s_0}/10}) \quad (\text{B.6})$$

and the sidelobe level is

$$S_d = S_0 + \text{SLD}, \quad (\text{B.7a})$$

where the sidelobe level for the un-degraded system is

$$S_0 = B_{s_0} - 10 \log[10^{D_1/10}(1 + 10^{B_{s_0}/10}) - 1] \quad (\text{B.7b})$$

and the sidelobe degradation is

$$\text{SLD} = 10 \log[(1 + (s_e/s_0)(1 - 2s_0)) / (1 - s_e s_0)]. \quad (\text{B.7c})$$

For later reference, we note that

$$\pi / \text{BW} = \text{DI}(1 + b_{s_0}) / (1 + s_e b_{s_0}). \quad (\text{B.8})$$

B.2. DERIVATION OF B_{s_d} AND B_m FOR AN ANISOTROPIC NOISE FIELD

For noise that is not isotropic the sidelobe/mainlobe ratio is determined from the two-valued beam pattern according to

$$b_{s_d} = s_d \left(\int_{\text{BW}_0} n_F(\theta'; \theta_s) d\theta' \right) / \left(\int_{\text{BW}_0} n_F(\theta'; \theta_s) d\theta' \right). \quad (\text{B.9})$$

From the definition of the angular noise distribution (Eq. (5) in the main text) and the fact that

$$N_0 = (1/\pi) \int_0^\pi n_F(\theta'; \theta_h) d\theta'$$

it follows that the integrals over the sidelobe sector and the mainlobe sector are related by

$$\pi N_0 = \int_{\text{BW}_0} n_F(\theta'; \theta_s) d\theta' + \int_{\text{BW}_0} n_F(\theta'; \theta_s) d\theta'. \quad (\text{B.10})$$

Substituting for the integral over the sidelobe sector from Eq. (B.10) into Eq. (B.9) and using the definition of the noise anisotropy (Eq. (6a) in the main text), we obtain

$$b_{s_d} = s_d ((\pi / \text{BW}) / a_N - 1). \quad (\text{B.11})$$

Using Eqs. (B.7a) and (B.5a) with $s_e = 0$ to write s_d in the form

$$s_d = 10^{\text{SLD}/10} (b_{s_0} / ((\pi / \text{BW}) - 1))$$

and substituting into Eq. (B.11) yields

$$b_{s_d} = 10^{\text{SLD}/10} (b_{s_0} / ((\pi / \text{BW}) - 1)) ((\pi / \text{BW}) / a_N - 1). \quad (\text{B.12})$$

The desired expression for the sidelobe/mainlobe ratio is obtained by rearranging Eq. (B.12) and expressing the results in a decibel scale. The result is

$$B_{s_d} = B_{s_0} + \text{SLD} - A_N + e(\pi / \text{BW}, a_N), \quad (\text{B.13a})$$

where

$$e(\pi / \text{BW}, a_N) = 10 \log \{ (\pi / \text{BW}) - a_N / ((\pi / \text{BW}) - 1) \} \quad (\text{B.13b})$$

and π / BW is given by Eq. (B.8). If $10 \log[\pi / \text{BW}] > 7$ dB and $A_N < 10 \log[\pi / \text{BW}] - 7$ dB, which is true for most cases of interest, the magnitude of $e(\pi / \text{BW}, a_N)$ is less than 1 dB and the sidelobe/mainlobe ratio is well approximated by the first three terms in Eq. (B.13a).

To obtain the expression for the mean beam for the two-valued beam pattern, we first use Eq. ((1) of the main text) in Eq. ((A.2) from Appendix A) to write the mean beam noise as

$$\bar{b}_T = \int_{\text{BW}_0} n_F(\theta'; \theta_s) d\theta' + s_d \int_{\text{BW}_0} n_F(\theta'; \theta_s) d\theta'. \quad (\text{B.14})$$

The integral over the sidelobe sector in Eq. (B.14) can be eliminated by using Eq. (B.9). The result is

$$\bar{b}_T = (1 + b_{s_d}) \int_{\text{BW}_0} n_F(\theta'; \theta_s) d\theta'. \quad (\text{B.15})$$

Using the definition of the noise anisotropy to replace the integral over the mainlobe sector in Eq. (B.15) results in

$$\bar{b}_T = \pi N_0 a_N (1 + b_{s_d}) / (\pi / \text{BW}). \quad (\text{B.16})$$

The desired expression for the mean beam noise, $B_m = 10 \log[\bar{b}_T]$ is obtained by using Eq. (B.8) to substitute for π / BW in Eq. (B.16) and expressing the results in decibels. The result is

$$B_m = 10 \log[\pi N_0] + A_N - \text{DI} + 10 \log[(1 + b_{s_d})(1 + s_e b_{s_0}) / (1 + b_{s_0})], \quad (\text{B.17})$$

where N_0 is expressed in a linear scale on a per radian basis. For realistic sidelobe degradations and noise anisotropies the sidelobe/mainlobe ratios are negligible, and the mean beam noise is well-approximated by the first three terms in Eq. (B.17).

We note in passing that since the beam pattern is normalized to a peak value of 0 dB, the array gain is simply the single hydrophone noise level, $10 \log[\pi N_0]$, minus the mean beam noise. Thus the array gain G_A is given by

$$G_A = \text{DI}_0 - A_N - 10 \log[(1 + b_{s_d})(1 + s_e b_{s_0}) / (1 + b_{s_0})]. \quad (\text{B.18})$$

Note that both the array gain and the sidelobe/mainlobe ratio (Eq. (13) in the main text) are decreasing functions of the noise anisotropy while the mean beam noise (Eq. (17) in the main text) is an increasing function of the noise anisotropy. At one extreme, where the noise in the sidelobe sector is zero, $A_N = \text{DI}$, $B_{s_d} = -\infty$, and $G_A = 0$ dB. At the other extreme, where the noise in the mainlobe sector is zero, $a_N = 0$, $B_{s_d} = +\infty$, and $G_A = \text{DI}$.

B.3. DERIVATION OF M_m AND M_s

To obtain the expression for M_m we use the fact that

$$D_0 = 1/\pi \int_0^\pi d_F(\theta'; \theta_h) d\theta' \quad (\text{B.19})$$

and the definition of the shipping anisotropy (Eq. (8) in the main text) to rewrite Eq. (A.3b) as

$$M_m = \pi D_0 a_S / (\pi / BW). \quad (\text{B.20})$$

The desired expression for M_m is obtained by substituting for π / BW from Eq. (B.8) into Eq. (B.20). The result is

$$M_m = 180 \times 10^{-R/10} (1 + s_e b_{s_0}) / (1 + b_{s_0}), \quad (\text{B.21a})$$

where

$$R = DI - A_S - 10 \log[D_0]; \quad (\text{B.21b})$$

D_0 is expressed on a per degree basis. To obtain the expression for M_s we use Eq. (6) and Eq. (19) from the main text) to write the integrals of $d_F(\theta'; \theta_h)$ over the sidelobe sector and the mainlobe sector as

$$\pi D_0 = \int_{BW_0} d_F(\theta'; \theta_s) d\theta' + \int_{BW_{0s}} d_F(\theta'; \theta_s) d\theta'. \quad (\text{B.22})$$

Substituting Eqs. (A.3a) and (A.3b) of Appendix A into Eq. (B.22) and using Eq. (B.21) results in

$$M_s = M_{sm} M_m, \quad (\text{B.23a})$$

where

$$M_{sm} = (\pi D_0 / M_m) - 1 \quad (\text{B.23b})$$

and D_0 is expressed in ships per radian.

Appendix C

Examples of shipping and noise environments

In this Appendix we identify certain shipping and noise environments that correspond to the three special cases identified in Sect. 2: (1) anisotropic noise— isotropic shipping; (2) anisotropic shipping— isotropic noise; and (3) identical shipping and noise anisotropies.

Environments that correspond to the first and the third cases can be identified immediately from the definitions of the two angular distributions (Eqs. 5a and 5b in the main text). For the first case, the shipping is isotropic whenever the spatial shipping density satisfies

$$D(r, \theta) = \begin{cases} D' & \text{for } r \in [R_1, R_2] \text{ and all } \theta \\ 0 & \text{otherwise.} \end{cases} \quad (C.1)$$

in which case the angular shipping distribution is independent of θ with the constant value of $R_e[\cos(R_1/R_e) - \cos(R_2/R_e)]$ ships per degree bearing where R_e is the radius of the earth in n.mi. For the shipping distribution of Eq. (C.1) the angular noise distribution will depend on θ whenever $\bar{T}(r, \theta)$ depends on θ . Thus an environment that results in anisotropic noise and isotropic shipping is one for which the shipping satisfies Eq. (C.1), and the mean transmission loss depends on bearing.

The third case, identical shipping and noise anisotropies, results whenever the product $\bar{S}(r, \theta) \times \bar{T}(r, \theta)$ is independent of r and θ over the region of non-zero shipping. This is seen by letting $\bar{S}(r, \theta) \times \bar{T}(r, \theta)$ be a constant in Eq. (5a) in the main text and noting that the result is proportional to the angular shipping distribution.

To provide an example example of an environment for the second case, anisotropic shipping— isotropic noise, we make the following simplifying assumptions: (1) the region containing the ships is sufficiently small that the differential element $dA(r)$ can be approximated by $r dr$; (2) the range set $R(\theta)$ is an interval with width $\Delta R(\theta)$ centered at the range $R_a(\theta)$; (3) the spatial shipping density $D(r, \theta)$ is constant over the region of non-zero shipping; and (4) the mean source level $\bar{S}(r, \theta)$ is independent of r and θ and the mean transmission loss is that of cylindrical spreading in all directions, i.e. $\bar{T}(r, \theta) = T_0/r$. It follows from the first three assumptions that the normalized angular shipping distribution, $d'(\theta) = d(\theta)/D_0$, can be written as

$$d'(\theta) = \Delta R(\theta)R_a(\theta)/\langle \Delta R(\theta)R_a(\theta) \rangle_\theta, \quad (C.2)$$

where $\langle \dots \rangle_\theta$ denotes the average over the angular sector of non-zero shipping. Similarly, it follows from all four assumptions that the normalized angular noise distribution $n'(\theta) = n(\theta)/N_0$, can be written as

$$n'(\theta) = \Delta R(\theta)/\langle \Delta R(\theta) \rangle_\theta. \quad (C.3)$$

Now assume that $\Delta R(\theta)$ is independent of bearing, i.e.

$$\Delta R(\theta) = \text{constant.} \quad (\text{C.4})$$

Then it follows from Eqs. (C.4) and (C.3) that the noise is isotropic and from Eqs. (C.4) and (C.2) that the normalized angular shipping distribution is given by

$$d'(\theta) = R_a(\theta) / \langle R_a(\theta) \rangle \theta. \quad (\text{C.5})$$

Thus, the anisotropic shipping—~~isotropic noise~~ case occurs whenever the ΔR is independent of θ and R_a is dependent on θ .

Other environments leading to the first and the third cases can be obtained in the setting described by the four assumptions. From Eqs. (C.2) and (C.3) it is seen that the anisotropic noise—~~isotropic shipping~~ case results whenever

$$\Delta R(\theta) \propto R_a(\theta)^{-1}, \quad (\text{C.6})$$

provided that $\Delta R(\theta)$ is not constant. Similarly, the identical anisotropy case results whenever R_a is independent of θ but ΔR is dependent on θ .

Finally we note that other cases can be obtained by assuming different relationships between ΔR and R_a . For example, if ΔR and R_a satisfy

$$\Delta R(\theta) \propto R_a(\theta)^{-2}, \quad (\text{C.7})$$

then

$$d'(\theta) = n'(\theta)^{-1}. \quad (\text{C.8})$$

Equation (C.8) corresponds to the case where the shipping anisotropy is the negative of the noise anisotropy.

Initial Distribution for SR-116

<u>Ministries of Defence</u>		SCNR Germany	1
JSPHQ Belgium	2	SCNR Greece	1
DND Canada	10	SCNR Italy	1
CHOD Denmark	8	SCNR Netherlands	1
MOD France	8	SCNR Norway	1
MOD Germany	15	SCNR Portugal	1
MOD Greece	11	SCNR Turkey	1
MOD Italy	10	SCNR UK	1
MOD Netherlands	12	SCNR US	2
CHOD Norway	10	French Delegate	1
MOD Portugal	2	SECGEN Rep. SCNR	1
MOD Spain	2	NAMILCOM Rep. SCNR	1
MOD Turkey	5	<u>National Liaison Officers</u>	
MOD UK	20	NLO Canada	1
SECDEF US	68	NLO Denmark	1
		NLO Germany	1
<u>NATO Authorities</u>		NLO Italy	1
Defence Planning Committee	3	NLO UK	1
NAMILCOM	2	NLO US	1
SACLANT	3	<u>NLR to SAACLANT</u>	
SAACLANTREPEUR	1	NLR Belgium	1
CINCWESTLANT/ COMOCEANLANT	1	NLR Canada	1
COMSTRIKFLTANT	1	NLR Denmark	1
CINCIBERLANT	1	NLR Germany	1
CINCEASTLANT	1	NLR Greece	1
COMSUBACLANT	1	NLR Italy	1
COMMAIREASTLANT	1	NLR Netherlands	1
SACEUR	2	NLR Norway	1
CINCNORTH	1	NLR Portugal	1
CINC SOUTH	1	NLR Turkey	1
COMNAVSOUTH	1	NLR UK	1
COMSTRIKFORSOUTH	1		
COMEDCENT	1		
COMMARARMED	1		
CINCHAN	3		
<u>SCNR for SAACLANTCEN</u>		Total external distribution	250
SCNR Belgium	1	SAACLANTCEN Library	10
SCNR Canada	1	Stock	20
SCNR Denmark	1		
		Total number of copies	280

END

DATE
FILMED

9 - 88